

POSSIBLE INCREASE IN EMITTANCE DUE TO NONLINEAR
COUPLING RESONANCES IN THE BOOSTER

Shoroku Ohnuma

July 15, 1974

I. Introduction

For the booster at Fermilab, nominal design values of the radial and the vertical tunes are 6.7 and 6.8, respectively. The operating point is therefore on the fourth-order, normal coupling resonance $2\nu_x + 2\nu_y = 27$ which is driven by the 27th harmonic component of a normal octupole field

$$\begin{aligned} B_x(x,y;s) &= (B_o''''(s)/6)(-y^3+3x^2y), \\ B_y(x,y;s) &= (B_o''''(s)/6)(x^3-3xy^2). \end{aligned} \quad (1)$$

Since the periodicity of the booster is 24, this harmonic component may arise only from random fluctuations in the octupole field from magnet to magnet or possibly from some special devices placed around the ring.

During January and February in 1973, a series of tune measurements were made at various energies. The measurement revealed, among other things, that the correction of the end field in F magnets was not perfect. As a result, the radial tune is significantly lower than the design value at high energies, where there is no simple way of making a substantial correction, and the momentum dependence of radial tune is an order of magnitude larger than expected.¹ The best estimate of tunes² and the chromaticity at high energies* are $\nu_x = 6.64$, $\nu_y = 6.79$, $\Delta\nu_x = -17(\Delta p/p)$ and

*The chromaticity depends somewhat on the correction sextupole current.

$\Delta v_y = 4(\Delta p/p)$. With the expected momentum spread $(\Delta p/p) = \pm 0.6 \times 10^{-3}$ in the beam, $\Delta v_x(\text{total}) = 0.02$ and $\Delta v_y(\text{total}) = 0.005$. In Fig. 1, this is indicated as a rectangle B and the design operating point is marked as A. Nearby third- and fourth-order resonances are shown by solid (normal resonances) and dashed (skew resonances) lines:

normal sextupole resonances	(1) $3v_x = 20$
	(2) $v_x + 2v_y = 20$
	(10) $2v_y - v_x = 7$
normal octupole resonances	(3) $4v_x = 27$
	(4) $4v_y = 27$
	(5) $2v_x + 2v_y = 27$
skew sextupole resonances	(6) $3v_y = 20$
	(7) $2v_x + v_y = 20$
skew octupole resonances	(8) $v_x + 3v_y = 27$
	(9) $3v_x + v_y = 27$
	(11) $3v_x - v_y = 13$.

Since these resonances are all driven by imperfection harmonics, their effects are expected to be negligible except for (8). Part of the beam represented by rectangle B is exactly on this resonance which will be driven by the 27th harmonic of a skew octupole field

$$\begin{aligned}
 B_x(x,y;s) &= (B_1''''(s)/6)(x^3 - 3xy^2), \\
 B_y(x,y;s) &= (B_1''''(s)/6)(y^3 - 3x^2y).
 \end{aligned}
 \tag{2}$$

Recently, it has been observed, at least in a qualitative manner,

that the vertical emittance of the beam increases when the radial emittance of the beam is made larger by a multi-turn injection³ and this may have contributed to the reduction* of the main-ring transmission efficiency. Since the beam intensity and the radial emittance of the beam are not controlled independently, one cannot exclude a vertical coherent oscillation induced by the self field of a high-intensity beam. This oscillation may eventually be smeared out by the tune spread, resulting in an increase in the vertical emittance. It is even conceivable that, during the long injection time of a multi-turn injection, the vertical position and angle of the injected beam fluctuate and cause an apparent increase in the emittance.

The purpose of this report is to demonstrate a possibility of increasing the vertical emittance through fourth-order coupling resonances $2\nu_x + 2\nu_y = 27$ and $\nu_x + 3\nu_y = 27$. Each resonance is treated separately as an isolated one so that there will be no multi-resonance effect.⁴ This is justified as the operating point here is very close to one resonance only and all resonances are expected to be weak. Another assumption is that the zeroth (average) harmonic component of normal octupole field is much smaller than the 27th harmonic of either normal octupole field or skew octupole field. In general, average octupole field (and certain other higher multipole fields) is important in creating outer stable regions in phase space.⁵ Since one is primarily interested in the nonlinear deformation of the inner stable area, the neglect of the effect of average octupole field should not be too serious a defect unless the

*The reduction was from 95% (single-turn injection) to 60% in April and to 80% in June, 1974.

average field is so large that there is no division of phase space into two or more regions.

Nonlinear betatron motion in the ideal booster has been investigated by S.C. Snowdon.⁶ A detailed analytical treatment of nonlinear resonances can be found in his report and in a report by L.C. Teng.⁷ Snowdon calculated the amplitude dependence of tunes due to $3\nu_x = 24$ and $\nu_x + 2\nu_y = 24$ resonances as well as due to the average octupole field. A discussion on the four-dimensional phase space for an isolated coupling resonance can be found, for example, in a report by A.G. Ruggiero.⁸

II. Invariant of the Motion

An isolated, nonlinear coupling resonance of the form

$$n_x \nu_x + n_y \nu_y = k; \quad n_x n_y \neq 0, \quad |n_x| + |n_y| \geq 3 \quad (3)$$

is treated here in the lowest-order approximation. In the Hamiltonian which describes the motion, only one nonlinear term with the slowest azimuthal variation is retained. Betatron motion of a particle is specified by

$$\begin{aligned} x &= \sqrt{W_x} \sqrt{\beta_x} \cos(\nu_x \phi_x + a_x), \\ y &= \sqrt{W_y} \sqrt{\beta_y} \cos(\nu_y \phi_y + a_y). \end{aligned} \quad (4)$$

Here, phase angles ϕ_x and ϕ_y , which increase by 2π every revolution, betatron oscillation parameters β_x and β_y and tunes ν_x and ν_y are all calculated from the linear property of the field. If there is no linear field, W_x , W_y , a_x and a_y are constant of the motion and the maximum value of W_x (W_y) in a beam multiplied by π is the radial (vertical) emittance. When nonlinear fields are introduced, one can describe the motion in terms of $(W_x, a_x, W_y, a_y; s)^*$ instead of

*It is customary to take $W_x/2$ and $W_y/2$ as canonical variables. However, this is not necessary for preserving the Hamiltonian formalism.

the original variables $(x, dx/ds, y, dy/ds; s)$. The new Hamiltonian is simply the nonlinear part of the original Hamiltonian.⁹ Another method developed by Sturrock⁵ adopts the Lagrangian formalism and calculates the change in $W_{x,y}$ and $a_{x,y}$ from an invariant integral which is called the perturbation characteristic function.¹⁰ In either formalism, one can construct two invariants of the coupled motion and the knowledge of these invariants is sufficient to find the range of the variation of W_x and W_y . What is not available is the information on each phase a_x and a_y and the change of dependent variables $W_{x,y}$ and $a_{x,y}$ as a function of the independent variable s . For example, the rate of growth for $W_{x,y}$ can be found only by solving equations of motion in some form. In this note, the formalism by Sturrock is adopted because of the simplicity of the expression for driving terms.

The operating point (v_x, v_y) under consideration is assumed to have the amount of detuning ϵ ,

$$n_x v_x + n_y v_y = k + \epsilon. \quad (5)$$

The nearest point on the resonance is (v_{x0}, v_{y0})

$$n_x v_{x0} + n_y v_{y0} = k \quad (6)$$

so that

$$\begin{aligned} \epsilon_x &\equiv v_x - v_{x0} = n_x \epsilon / (n_x^2 + n_y^2) \\ \epsilon_y &\equiv v_y - v_{y0} = n_y \epsilon / (n_x^2 + n_y^2). \end{aligned} \quad (7)$$

Two invariants of the coupled motion are

$$\begin{aligned} \Phi_x &\equiv DK_x^m K_y^n \cos(n_x a_x + n_y a_y + \delta) - \epsilon K_x^2 / (2n_x), \\ \Phi_y &\equiv DK_x^m K_y^n \cos(n_x a_x + n_y a_y + \delta) - \epsilon K_y^2 / (2n_y) \end{aligned} \quad (8)$$

where $K_{x,y} = \sqrt{W_{x,y}}$, $m = |n_x|$ and $n = |n_y|$. The amplitude and phase

of the driving term are D and δ , respectively, and these must be evaluated using linear motion parameters β_{x0} , β_{y0} , ϕ_{x0} and ϕ_{y0} that belong to the point (v_{x0}, v_{y0}) on the resonance. However, as $|\epsilon| \ll 1$, one may substitute linear motion parameters of the operating point (v_x, v_y) . By taking the difference of two invariants, one can get another invariant which is more familiar,

$$K_x^2/n_x - K_y^2/n_y = \text{invariant}$$

or

$$n_y W_x - n_x W_y = \text{invariant.} \quad (9)$$

For the motion to be real, K_x and K_y must vary such that $|\cos(n_x a_x + n_y a_y + \delta)| \leq 1$ with constant values of ϕ_x and ϕ_y . Values of $\phi_{x,y}$ are of course specified by the initial condition. In the following section, two coupling resonances, $2v_x + 2v_y = k$ and $v_x + 3v_y = k$, are studied in detail.

III. Nonlinear Deformation

A. $2v_x + 2v_y = k + \epsilon$; $n_x = n_y = 2$.

It is unlikely that the operating point of the booster is very close to this resonance during the acceleration. Nevertheless, it is interesting to see the possible deformation arising from this resonance and compare with the deformation due to $v_x + 3v_y = k$. Also, the expression for two invariants of this resonance is amenable to a simple algebraic treatment.

The driving term is

$$D \exp(i\delta) = (1/64\pi) \int ds [B'_0 / (B\rho)] \beta_{x0} \beta_{y0} \exp[i(2v_{x0} \phi_{x0} + 2v_{y0} \phi_{y0})]. \quad (10)$$

One can rewrite two invariants as

$$\begin{aligned}\lambda &= u^2 v^2 w + u^2, \\ \mu &= u^2 v^2 w + v^2\end{aligned}\quad (11)$$

where

$$\begin{aligned}u &= 2\sqrt{D/|\epsilon|} K_x, \\ v &= 2\sqrt{D/|\epsilon|} K_y, \\ w &= -(|\epsilon|/\epsilon)\cos(2a_x + 2a_y + \delta), \\ \lambda &= -(16|\epsilon|/\epsilon^3)D\phi_x, \\ \mu &= -(16|\epsilon|/\epsilon^3)D\phi_y.\end{aligned}\quad (12)$$

Two-dimensional relation (11) can be reduced to a one-dimensional form by eliminating the vertical "amplitude" v ,

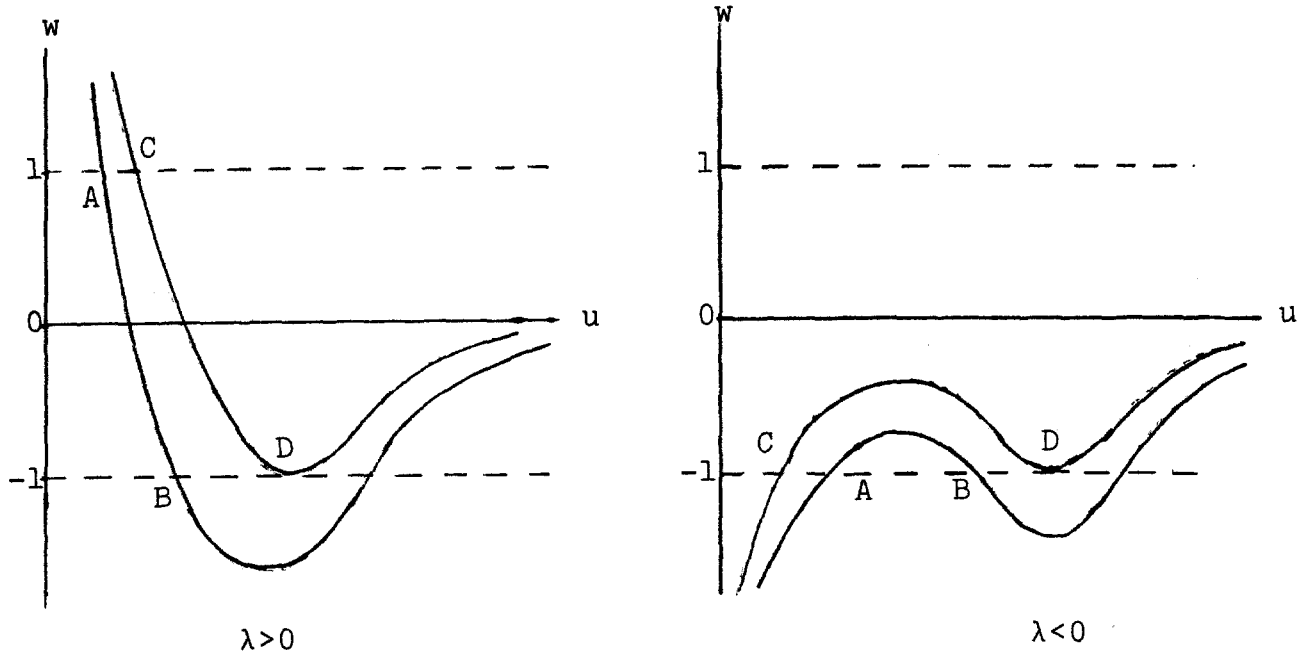
$$w = \frac{\lambda - u^2}{u^2(u^2 - \lambda + \mu)} \quad (13)$$

where $u^2 - \lambda + \mu \equiv v^2$ must always be positive. From the asymptotic and the limiting behaviors of $w(u)$,

$$\begin{aligned}w &\rightarrow -u^{-2} \text{ as } u \rightarrow \infty, \\ w &\rightarrow \lambda u^{-2}(\mu - \lambda)^{-1} \text{ as } u \rightarrow 0 \text{ } (\lambda < \mu), \\ w &\rightarrow \mu(\lambda - \mu)^{-1} (u^2 - \lambda + \mu)^{-1} \text{ as } u \rightarrow \sqrt{\lambda - \mu} \text{ } (\lambda > \mu),\end{aligned}$$

one can see that the condition $|w| \leq 1$ gives a bounded region of u only when turning points of $w(u)$, $dw/du = 0$, exist outside the region $|w(u)| \leq 1$. The deformation of the stable area is obtained by the limiting condition

$$dw/dn = 0 \text{ at } w = +1 \text{ or } -1.$$



In the figures above, the motion is stable between A and B. The motion between C and D is the limiting case. From (13)

$$dw/du = 2u^{-3}(u^2 - \lambda + \mu)^{-2}(u^4 - 2\lambda u^2 + \lambda^2 - \lambda\mu) \quad (14)$$

and $dw/du = 0$ at $u = u_M$,

$$u_M^2 = \lambda \pm \sqrt{\lambda\mu} \quad (15)$$

From the requirement that both u_M^2 and $v_M^2 \equiv u_M^2 - \lambda + \mu$ must be real and non-negative, the only solution for $dw/du = 0$ is

$$u_M^2 = \lambda + \sqrt{\lambda\mu} \quad \text{with } \lambda \geq 0 \text{ and } \mu \geq 0. \quad (16)$$

The maximum deformation may be found by taking the initial values u_0 and v_0 at $w = +1$ and using $w(u_M) = -1$ as an additional condition. It is easy to see that

$$u_M^2 = \lambda + \sqrt{\lambda\mu} = \sqrt{\lambda} \quad (17)$$

$$v_M^2 = u_M^2 - \lambda + \mu = 1 - \sqrt{\lambda} \quad (18)$$

so that

$$u_M^2 + v_M^2 = 1. \quad (19)$$

From (17), $\sqrt{\lambda} + \sqrt{\mu} = 1$ or, with $\lambda = u_o^2 v_o^2 + u_o^2$ and $\mu = u_o^2 v_o^2 + v_o^2$,

$$v_o^2 = (1 + 3u_o^2) - \sqrt{(1 + 3u_o^2)^2 - (1 - u_o^2)^2}. \quad (20)$$

Two limiting curves in (u, v) plane, (19) and (20), are shown in Fig. 2 which is the projection of four-dimensional phase space regions. As projected, the phase space is made of three areas: (1) area bounded by $u=0$, $v=0$ and Eq. (20). Any point in this area is always stable and the maximum possible excursion is given by (u_M, v_M) curve, Eq. (19). (2) area bounded by Eqs. (19) and (20). A point in this area may or may not be stable depending on the value of a phase combination $(2a_x + 2a_y + \delta)$. (3) area outside (u_M, v_M) curve. Points are all unstable regardless of their phase values. In all cases, the motion of a point is always along a hyperbola, $u^2 - v^2 = \text{constant}$, which is equivalent to the relation (9). It should be emphasized again that Fig. 2 does not give any information on phases which, however, is not needed for the present purpose.

In order for all particles in a beam to be stable, they must be initially confined within the central stable area. Distribution of particles in phases a_x and a_y should be uniform but the distribution in amplitudes u and v depends on how the beam is formed. For the booster, the vertical emittance is independent of the mode of injection but the radial emittance increases when a multi-turn injector is used. It is customary to take an elliptic boundary

$$W_x/r + W_y \leq W_o \quad (21)$$

where πW_0 and $\pi r W_0$ are, respectively, the vertical and radial emittance.* For single-turn injection, r is unity and for four-turn injection, $r \geq 4$. Eq. (21) is an ellipse in (u, v) plane

$$u^2/r + v^2 \leq A \equiv (4D/|\epsilon|)W_0. \quad (22)$$

For the largest possible ellipse within the stable area,

$$A = (-1 - r + \sqrt{1+6r+r^2})/(2r) \quad (23)$$

and it touches the boundary curve, Eq. (20), at (u_0, v_0) ,

$$u_0^2 = (-1 + \frac{1 + 3r}{\sqrt{1+6r+r^2}})/2, \quad (24)$$

$$v_0^2 = (-1 + \frac{3 + r}{\sqrt{1+6r+r^2}})/2.$$

The largest ellipse is shown in Fig. 2 for $r = 1$ and 4 . If $w = +1$, the point (u_0, v_0) given by (24) can eventually move to (u_M, v_M) on the circle, Eq. (19), when w becomes -1 ,

$$u_M^2 = (1 + \frac{r - 1}{\sqrt{1+6r+r^2}})/2, \quad (25)$$

$$v_M^2 = (1 - \frac{r - 1}{\sqrt{1+6r+r^2}})/2.$$

These points are marked in Fig. 2 for $r = 1 - 4$. For other points on the ellipse (22), one can calculate the largest possible amplitude with the following procedures. Take a point (u_i, v_i) on the boundary of the ellipse and calculate λ and μ from (11) with $w = +1$. Increase u and calculate w from (13) until $w = -1$ at $u = u_f$.

*This is a mathematical expression of a statement, "Beam is always round", supposedly made by Ken Green.

The final (largest) value of v is then $v_f = \sqrt{u_f^2 - \lambda + \mu}$. The resulting curve for $r = 4$ is plotted in Fig. 2 as a dotted curve.

The relative increase in the radial emittance, $u_M^2/(rA)$, is not large, the maximum value being 1.21 for $r = 1$. As r increases, it approaches unity. On the other hand, the relative increase in the vertical emittance, v_M^2/A , goes up with r , approaching two asymptotically:

$r =$	1	2	3	4	∞
$v_M^2/A =$	1.21	1.35	1.44	1.52	2.00 .

In reality, the particle distribution is not uniform within the ellipse and the boundaries shown in Fig. 2 apply only for those particles with $w(\text{initial}) = +1$. "Visible" emittance increase may therefore be much smaller than values indicated above.

B. $v_x + 3v_y = k + \epsilon$; $n_x = 1, n_y = 3$.

At high energies, this resonance is expected to be the closest one to the operating point. The procedure for finding the maximum possible deformation of phase space is identical to what is used for $2v_x + 2v_y = k$ but a certain amount of numerical work is required for this case.

The driving term arising from skew octupole field, Eq. (2), is

$$D \exp(i\delta) = -(1/96\pi) \int ds [B_1'''(s)/(B\rho)] \beta_{x0}^{1/2} \beta_{y0}^{3/2} \times \exp[i(v_{x0}\phi_{x0} + 3v_{y0}\phi_{y0})]. \quad (26)$$

Two invariants are

$$\begin{aligned} \lambda &= uv^3w + u^2, \\ \mu &= uv^3w + v^2 \end{aligned} \quad (27)$$

with

$$\begin{aligned}
 u &= (108)^{\frac{1}{4}} \sqrt{D/|\epsilon|} K_x \\
 v &= (12)^{\frac{1}{4}} \sqrt{D/|\epsilon|} K_y, \\
 w &= -(|\epsilon|/\epsilon) \cos(a_x + 3a_y + \delta), \\
 \lambda &= -(12\sqrt{3} |\epsilon|/\epsilon^3) D\Phi_x, \\
 \mu &= -(12\sqrt{3} |\epsilon|/\epsilon^3) D\Phi_y.
 \end{aligned} \tag{28}$$

From these,

$$w = \frac{\lambda - u^2}{u(u^2 - \lambda + \mu)^{3/2}} \tag{29}$$

where $u^2 - \lambda + \mu \equiv v^2$ must be positive.

In (λ, μ) plane, there are now two regions in which real solutions (u_M, v_M) of $dw/du = 0$ exist.

(a) $\lambda \geq 0$ and $\mu \geq 0$

The boundary can be obtained by the conditions $(u_o, v_o, w = +1)$ and $(u_M, v_M, w = -1)$ where

$$u_M^2 = [(3\lambda + \mu) + \sqrt{\lambda^2 + 14\lambda\mu + \mu^2}]/4 . \tag{30}$$

This is analogous to the situation for $2v_x + 2v_y = k$.

(b) $\lambda < 0$ and $\lambda + \xi\mu \geq 0$ where $\xi = 7 - \sqrt{48}$.

Two values of u_M are possible.

$$u_M^2 = [(3\lambda + \mu) \pm \sqrt{\lambda^2 + 14\lambda\mu + \mu^2}]/4 . \tag{31}$$

However, for the solution with minus sign, $|w|$ is less than one. Boundaries are specified by $(u_o, v_o, w = -1)$ and $(u_M, v_M, w = -1)$ with plus sign in (31). The situation is depicted in the right-hand picture on p.8.

Boundary curves in (u, v) plane have been obtained numerically from (29), (30) and (31) with plus sign and they are shown in Fig. 3.

Boundaries (u_o, v_o) and (u_M, v_M) are for (a) whereas boundaries (u_o', v_o') and (u_M', v_M') are for (b).* A point between A and B with $w = -1$ moves along a hyperbola until it reaches a point between A' and B, again with $w = -1$. The point B represents the limiting case, $u_o' = u_M'$ and $v_o' = v_M'$. Coordinates of these special points are

$$A: u^2 = 0, v^2 = 2/(3\sqrt{3})$$

$$B: u^2 = (1 - 3\xi)\mu/4, v^2 = (5 + \xi)\mu/4$$

$$\text{with } \mu = 4(1 + \xi)(1 - 3\xi)^{-1/2}(5 + \xi)^{-3/2}$$

$$A': u^2 = 1/(3\sqrt{3}), v^2 = 1/\sqrt{3}.$$

The projected phase space is again divided into three regions as discussed for $2v_x + 2v_y = k$.

In (u, v) plane, the elliptic boundary of a beam, Eq. (21), takes the form

$$u^2/(3r) + v^2 \leq A \equiv (2\sqrt{3} D/|\epsilon|)W_o. \quad (32)$$

The largest ellipse for $r = 1$ and 4, points of the largest distortion for $r = 1 - 4$, and the maximum possible boundary of the beam for $r = 4$ are all plotted in Fig. 3. These points and boundaries are identical in their meanings to those in Fig. 2 but simple algebraic expressions for them are not available. Numerical results used for plotting them are given in Table 1 from which one can calculate the relative increase in the vertical emittance,

$v_M^2/A:$	r	1	2	3	4
v_M^2/A		1.81	1.88	1.91	1.93

*There is an error in the paper by Sturrock, ref. 5, pp. 176 - 179. For the resonance $v_x + 2v_y = k$, he missed the existence of the region (b), with $\xi = 1/8$, in (λ, μ) plane. As a result, he was compelled to make a conclusion that there are points of arbitrarily small amplitudes u and v which lie outside the stable region. The case is properly treated in Lysenko's paper, ref. 9.

Note that this resonance does not give rise to any increase in the radial emittance when $r \geq 1$. On the other hand, as far as the increase in the vertical emittance is concerned, it is more dangerous than $2v_x + 2v_y = k$.

It is probably more interesting to see how much increase one must expect in the vertical emittance when the beam occupies an area which is smaller than the limiting (maximum) ellipse. The beam boundary is now written as

$$u^2/(3r) + v^2 = fA_1 \quad (33)$$

where f is less than unity and $A_1 (= 0.2761$ from Table 1) is A of Eq. (32) for $r = 1$. For $r > 1$, the beam is stable if fA_1 does not exceed A that corresponds to that value of r :

$$f(r=2) \leq (0.2252/0.2761) = 0.816,$$

$$f(r=3) \leq (0.1945/0.2761) = 0.704,$$

$$f(r=4) \leq (0.1736/0.2761) = 0.629$$

The maximum increase in the vertical emittance is shown in Fig. 4 as a function of f . For example, if the strength of driving term D , the amount of detuning $|\epsilon|$ and the vertical emittance πW_0 are such that

$$(2\sqrt{3} D/|\epsilon|)W_0 = 0.7 A_1,$$

the maximum increase in the vertical emittance is negligible for $r = 1$ (single-turn injection, radial emittance = πW_0) but it is significant for $r \geq 3$ (multi-turn injection, radial emittance $\geq 3\pi W_0$). The vertical emittance growth will therefore become more "visible" as the radial emittance is increased.

IV. Concluding Remarks

It is not possible to make a quantitative statement beyond what is presented here without knowing the strength of the driving

term. One may be able to measure this strength by placing the operating point in the rectangle B in Fig. 1 and measuring the vertical emittance growth as a function of the radial emittance. This, however, is possible only for the coasting (200 MeV) beam. Since the strength of trim quadrupoles is not programmable, the operating point will move out of the rectangle, that is, away from the resonance when the beam is accelerated.

Effects of the average octupole field, which are neglected here, may affect the amount of deformation. However, the method in this report is still applicable if terms of the form

$$AK_x^4 + BK_x^2 K_y^2 + CK_y^4$$

are included in the expressions for both Φ_x and Φ_y , Eq. (8).

Here

$$A = -(1/128\pi) \oint ds (B_o''''/B\rho) \beta_x^2,$$

$$B = (1/32\pi) \oint ds (B_o''''/B\rho) \beta_x \beta_y,$$

and

$$C = -(1/128\pi) \oint ds (B_o''''/B\rho) \beta_y^2. \quad (34)$$

Numerical calculations are then unavoidable and the picture in (λ, μ) plane and in (u, v) plane will be more complex.

The treatment given here is entirely static and no effect of crossing a resonance has been considered. It is quite conceivable that crossing one or more resonances during the acceleration contributes significantly to the increase in the emittance.^{5,9,11}

Table 1

For the resonance $v_x + 3v_y = k$, the largest beam ellipse in (u, v) plane

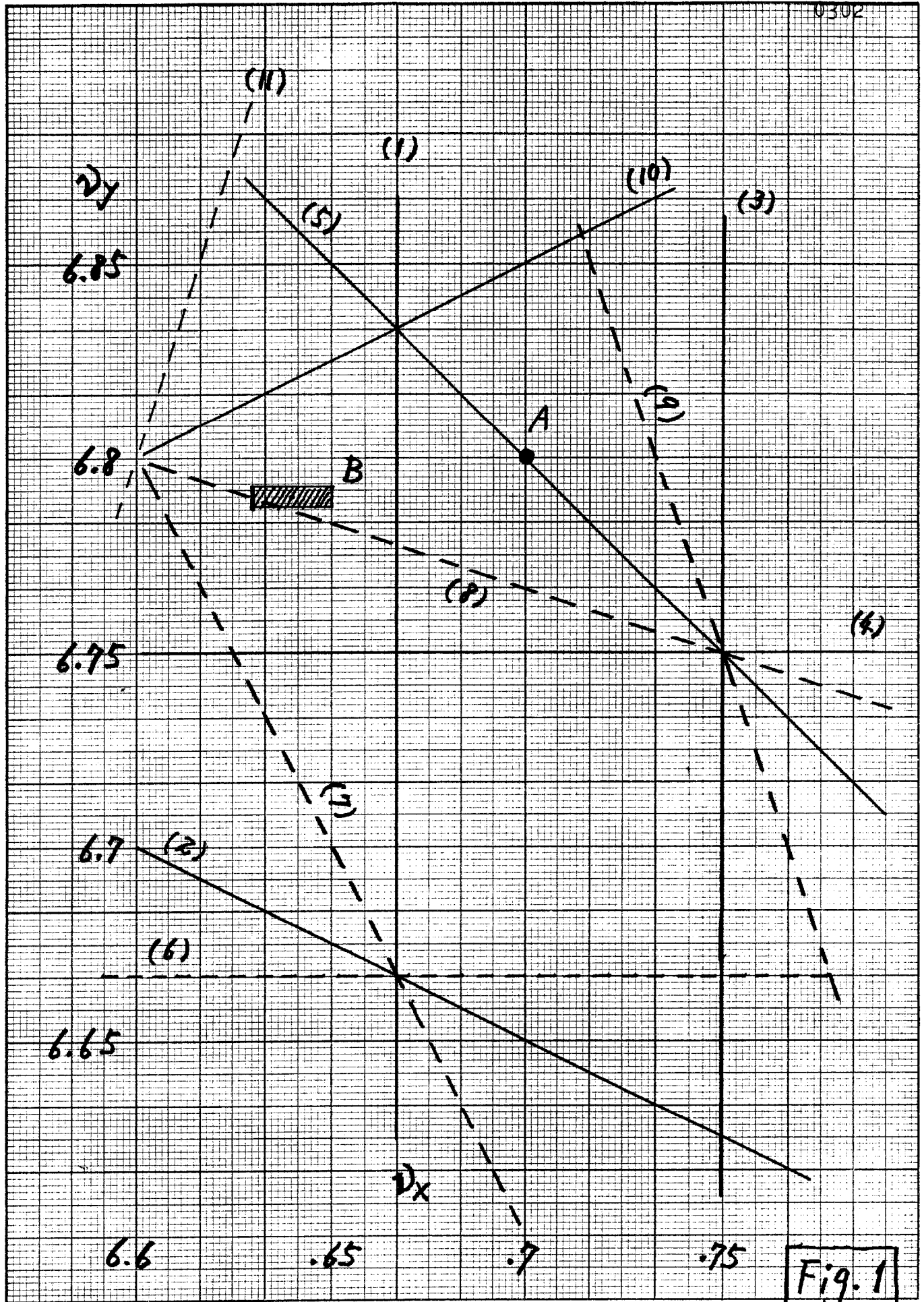
$$u^2/(3r) + v^2 = A$$

touches the boundary of the central stable area at (u_o, v_o) . This point can move up to (u_M, v_M) on the outer boundary curve. See Fig. 3.

r	1	2	3	4
A	.2761	.2252	.1945	.1736
u_o	.455	.682	.823	.925
v_o	.455	.384	.345	.320
u_M	.707	.861	.964	1.044
v_M	.707	.651	.610	.579

References

1. It is unfortunate that there is no report on this subject although various data have been made available by the booster group (E. Gray, E. Hubbard and R. Peters) and by T. Collins.
2. R. Peters, private communication
3. F. Mills and R. Stiening, private communications.
4. There is no rigorous analytical treatment of two or more simultaneous resonances. Only exception is the work by Meier and Symon for $\nu_x + 2\nu_y = N$ and $\nu_x - \nu_y = 0$. Their formalism is difficult to extend to more general cases. H. Meier and K.R. Symon, Proceedings of the International Conference on High-Energy Accelerators and Instrumentation, CERN 1959, p. 253.
5. See, for example, P.A. Sturrock, Annals of Physics 3, 113 (1958); in particular, pp. 132-138 and pp. 151-156.
6. S.C. Snowdon, FN-190, May 28, 1969.
7. L.C. Teng, FN-183, March 27, 1969.
8. A.G. Ruggiero, FN-258, April 24, 1974.
9. W.P. Lysenko, Particle Accelerators 5, 1 (1973). Note that his "angle" variable is different from the usual angle of the action-angle variables. In the usual treatment, the new Hamiltonian still contains a linear part, $\nu_x W_x/2 + \nu_y W_y/2$. See ref. 6 and 7.
10. P.A. Sturrock, Static and Dynamic Electron Optics, Cambridge University Press, 1955.
11. A.W. Chao and M. Month, BNL-18860 (CRISP 74-9), April 22, 1974.



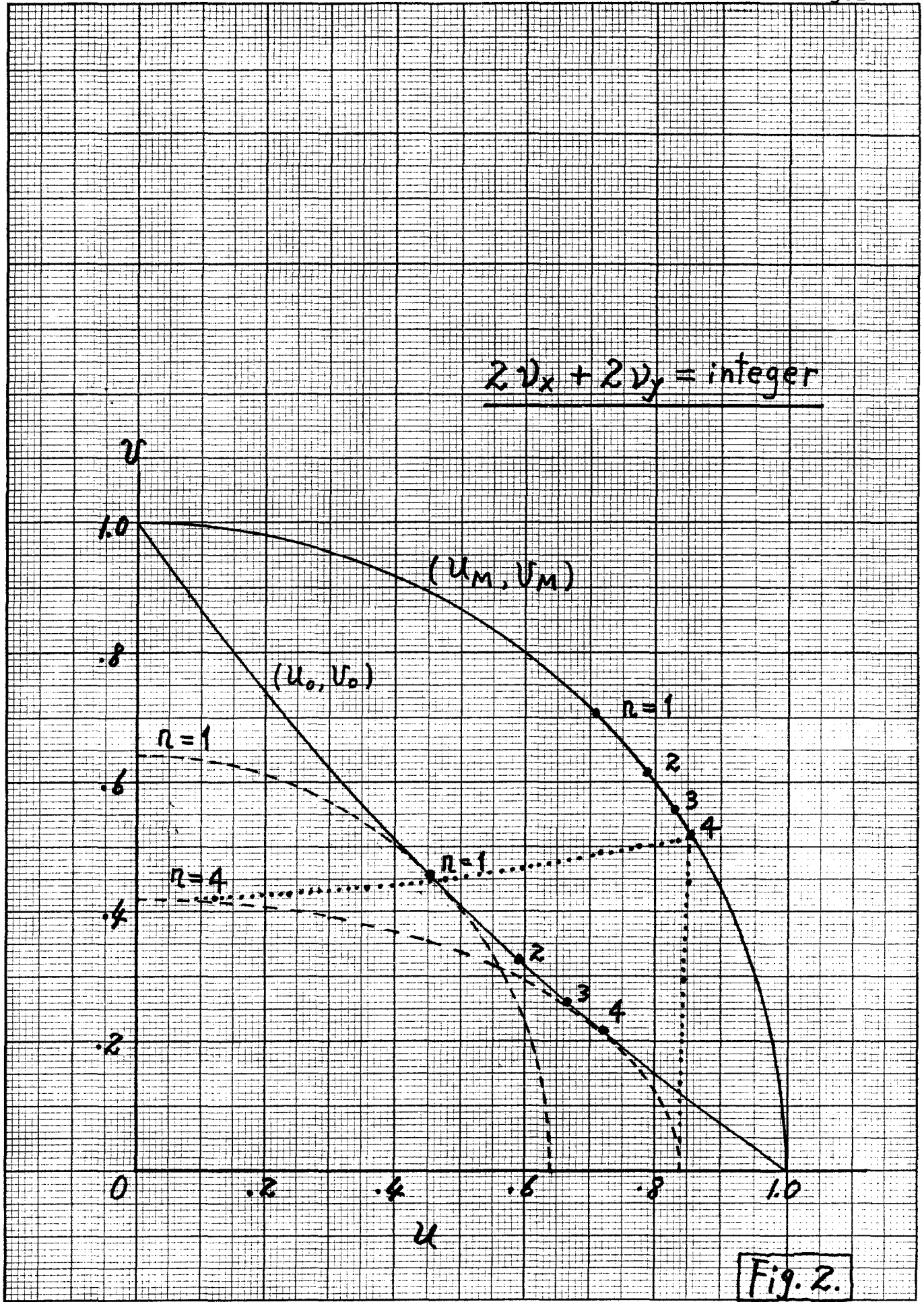


Fig. 2.

Fig. 3

$2x + 32y = \text{integer}$

